Use of Extra Measurements for Systems with Unstable Zero Dynamics

Einar Hauge

Department of Engineering Cybernetics
Norwegian University of Science and Technology
2006

NTNU
Norwegian University of
Science and Technology

Faculty of Informatics, Mathematics
and Electrical Engineering

Department of Engineering Cybernetics

PROSJEKTOPPGAVE

Kandidatens navn:	Einar Hauge
Veileder:	Professor Sigurd Skogestad
Veileder ved Institutt for teknisk kybernetikk :	Professor Morten Hovd
Fag:	Teknisk kybernetikk
Title:	Use of Extra Measurements for Systems with Unstable Zero Dynamics
Tittel:	Bruk av ekstra målinger for systemer med ustabil nullpunktsdynamikk.

Prosjektbeskrivelse:

Use of extra measurements for systems with unstable zero dynamics
The project is motivated by anti-slug control using topside measurements, where stabilization is difficult because both the pole and zero dynamics are unstable (RHP-poles and zeros). The objective is to find whether one can use extra measurements with RHP-zeros at different locations, and in particular to quantify the performance limitations. First, "academic" cases with real poles and zeros, complex RHP-poles with real RHP-zeros, and complex RHP-poles with complex RHP-zeros. Finally, a model representing anti-slug control will be studied.

Figure 0.1

Preface

This report is the result of the mandatory project in the 5th year of my M.Sc. education at Norwegian University of Science and Technology. The purpose of this project was to analyze use of extra measurements in systems with unstable zero dynamics. This was motivated by the fact that slug flow is characterized by this kind of dynamics.

I want to thank my supervisor professor Sigurd Skogestad at the Department of Chemical Engineering for his valuable support and advice. I would also like to thank PhD-student Heidi Sivertsen for her help.

Trondheim, Norway, December 2006

Einar Hauge

Abstract

Using topside measurements for stabilizing riser-induced slug flow is hard due to unstable pole and zero dynamics. At least when trying to use SISO-control. It is well known from linear system theory that linear combination of measurements can be used for moving zeros. However, there is a contradiction that two performance limited measurements with unstable zero dynamics, can be combined, and by this combination remove the limitation completely.

Using linear combinations of measurements is in this report first investigated on a simple process example with two measurements, both with unstable pole and zero dynamics. This approach worked well on this process, however it could be concluded that using such a linear combination was exposed to model-uncertainty. In addition to this, it was shown that having very similar measurements would worsen the exposure of this type of uncertainty. Physical this means that if you have two measurements that actually measure the same, moving the zeros is impossible.

The two measurements in the simple process had only one zero each. Moving the zero in a linear combination approach was therefore easy. The topside measurements from the slug flow problem have two or more zeros. This implicates that controlling how the zeros are moved is much more difficult. And it is pointed out that this is a limitation in itself.

Using a linear combination of the density (ρ_T) and the differential pressure over the choke-valve (DP) was unable to move all the zeros into the left half-plane. Using a combination with DP and W was on the other hand a successful approach in terms of moving all the zeros into the left half-plane. This was also the case with a linear combination of ρ_T and W.

Contents

1 Motivation

Slug flow in multiphase pipelines is a severe problem for the oil industry. Slug flow is an unstable flow regime in which the gas and liquid flows separately through the pipeline. This irregular flow causes poor separation, limits production capacity and causes flaring. The slugs can be so large that they even fill up the down stream separator completely. [2]

Slug flow is often subdivided into groups based on which physical phenomena they arise from. These are hydrodynamic slugging, terrain slugging, transient slugging and riser slugging. [2]

Hydrodynamic slugging is created because of liquid waves forming on the gas-liquid interface. When these waves grow so large that they fill the cross-section of the pipeline, the slugs are formed. Terrain slugging is formed by rough seafloor, where slug of liquids are formed at low-points. Transient slugging are induced because of changes in operating conditions.

The focus in this report, however, will be on riser-slugging. Riser-slugging is induced by liquid filling up at the bottom of the riser, thus preventing the gas from flowing into the riser. The pressure upstream the liquid is then building up eventually causing the liquid slug to blow up the riser. This process will repeat itself, causing an oscillatory flow regime. See figure 1.1 for a typical riser.

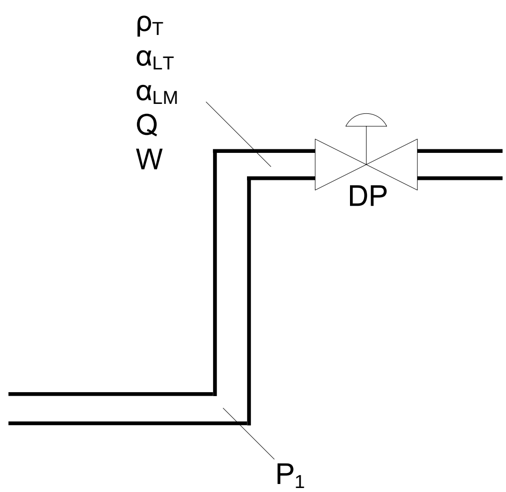

Figure 1.1

Often this problem has been dealt with using what is commonly known as a slug-catcher. A slug-catcher is a physical structure which tries to smooth out the incoming multiphase flow. These structures can be quite large, and is often unwanted from a weight and size perspective.

Another way to avoid the unwanted oscillatory flow regime is to reduce the opening of the choke valve below a critical value, $z < z_{crit}$. A simple approach would then be to make sure that the valve-opening would never be larger than this value. However, this is undesirable since a small opening of the choke-valve would mean poor productivity and lesser income.

However, another way to address this problem is using control theory and active feedback to control the choke-valve and by then smooth out the flow variations. This would be an approach which does not impose large physical structures or limit the economic outcome.

It is already shown by [5] that using the riser base pressure P_1 defined in figure 1.1 would stabilize the flow. However, it would be much more practical to use only topside measurements, such that installing subsea equipment could be avoided. A problem with most of these topside measurements, which will be further analyzed in this report, is that controllability is limited because of unstable zero dynamics (RHP-zeros). The only measurement which does not contain any right half-plane zeros is the volume flow Q. On the other hand, it is impossible to use this measurement alone, because of low steady-state gain which would cause drifting.

One approach which has been tried in [3] is cascade control with the volume flow Q in an inner stabilizing loop, and using two alternatives, the position of the choke-valve z and the topside pressure P_2 in an outer loop for performance. P_2 would here correspond to the absolute pressure topside, in stead of DP pressure which is shown in figure 1.1

Another interesting approach is to try to use linear combinations of the topside measurements to move the performance limiting right half-plane zeros. This has also been analyzed in [3], and this is the approach which will be investigated further in this report. The topside measurements which will be analyzed in this report are shown in figure 1.1. The mathematical model which is used for describing the slug flow is a simplified 3-state model for two-phase flow outlined in [5]. This model is restated in appendix A.

2 Theory

This chapter states the theory which will be used in the subsequent chapters. First some control theory notation will be described, before a mathematical description of the performance limitations will be presented. Next a method for monitoring the placement of the zeros and some theorems for bandwidth requirements are stated.

2.1 Block diagram

There will be used typical control theory notation, as the sensitivity S and the complementary sensitivity T. These transfer functions are defined according to the block-diagram given below.

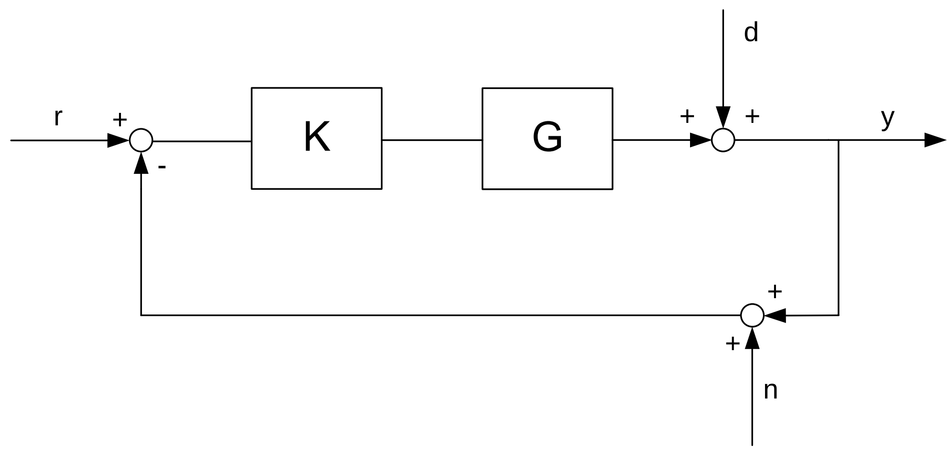

Figure 2.1: A typical control structure

where

$$y(s) = T(s)r(s) + S(s)d(s) - T(s)n(s) \tag{2.1}$$

and

$$u(s) = K(s)S(s)(r(s) - d(s) - n(s)) \tag{2.2}$$

$T(s)$ and $S(s)$ are defined as:

$$S = \frac{1}{1+GK}, T = \frac{GK}{1+GK} \tag{2.3}$$

$$L(s) = GK \tag{2.4}$$

2.2 Mathematical description of control limitations due to unstable zero dynamics

The slugging problematic is exposed to severe performance and stability limitations due to both unstable pole-and zero dynamics. These limitations can be described mathematical by what is called the second waterbed formula. The following theorem can be found in [4].

Theorem 2.1 *Suppose that the open-loop transfer function $L(s)$ has a single real RHP-zero or a complex conjugate pair of zeros $z = x \pm jy$, and has N_p RHP-poles, p_i. Let $\bar{p}_i$ denotes the complex conjugate of p_i. Then for closed-loop stability the sensitivity function must satisfy:*

$$\int_0^\infty ln|S(j\omega)| \cdot w(z,\omega)\, d\omega = \pi \cdot \prod_{i=1}^{N_p} \left| \frac{p_i + z}{\bar{p}_i - z} \right| \tag{2.5}$$

where

$$w(z,\omega) = \frac{2z}{z^2 + \omega^2}$$

The sensitivity (S) is the closed-loop transfer function from disturbance (d) to the output y. For performance we want the sensitivity to be small at low frequencies for disturbance rejection. A large peak in the sensitivity is therefore unwanted from a disturbance rejection perspective. The right hand side of equation (2.5) says that the integral will have a larger value if the RHP zeros and RHP poles are close to each other. Thus a large peak on the sensitivity is unavoidable. Below are theorems (given in [4]) which give lower bounds on the sensitivity S, the complementary sensitivity T and KS.

Theorem 2.2 *For closed-loop stability the sensitivity function must satisfy for each RHP-zero of $G(s)$ the following bound on the sensitivity. p_i denote the N_p RHP-poles of $G(s)$.*

$$\|S\|_\infty \geq \prod_{i=1}^{N_p} \frac{|z + p_i|}{|z - p_i|} \tag{2.6}$$

Theorem 2.3 *The complementary sensitivity T must satisfy for each RHP-pole p of G(s)*

$$\|T\|_\infty \geq \prod_{j=1}^{N_z} \frac{|z_j + p|}{|z_j - p|} \tag{2.7}$$

where z_j denote the N_z RHP-zeros of $G(s)$.

Theorem 2.4

$$\|KS\|_\infty \geq \frac{1}{\sigma_H(U(G)^*)} \tag{2.8}$$

where σ_H denote the smallest Hankel singular value and $U(G)^*$ is the mirror image of the anti-stable part of G.

2.3 Algebraic criterion for the placement of zeros

As mentioned earlier, this report investigates the placement of the zeros in the context of linear combination of measurements. The zero polynomial can be written in the form:

$$P_z(s) = s^n + \phi_{n-1}s^{n-1} + \ldots + \phi_1 s + \phi_0 = \sum_{i=0}^{n} \phi_i s^i \tag{2.9}$$

The zeros are found by solving:

$$P_z(s) = 0 \tag{2.10}$$

In this context we would like to have all the zeros far into the left half-plane for the purpose of stabilization and performance of the control system. Routh's criterion, defined in a theorem below, helps addressing this problem and gives sufficient condition for making sure that all the zeros are to the left of the imaginary axis. Usually, Routh's criterion is in control theory applied for investigation of closed-loop stability. It is here, however, used for the purpose of monitoring the location of the zeros of the open-loop system.

Theorem 2.5 ***Routh's criterion.***
Defining the zero polynomial as $P_z(s) = \sum_{i=0}^{n} \phi_i s^i$. A necessary condition for making sure that the zeros are all negative (in LHP), all ϕ_i's need to have the same sign. A sufficient condition is that all the coefficients in the left column in the table below have the same sign.

$$
\begin{array}{cccc}
\phi_n & \phi_{n-2} & \cdots & \phi_1 \\
\phi_{n-1} & \phi_{n-3} & \cdots & \phi_0 \\
\beta_{n-1} & \beta_{n-3} & \cdots & \\
\xi_{n-1} & \xi_{n-3} & \cdots & \\
\cdot & & & \\
\cdot & & & \\
\cdot & & & \\
\sigma_{n-1} & \sigma_{n-3} & & \\
\eta_{n-1} & & & \\
\omega_{n-1} & & &
\end{array}
$$

Table 2.1

The new coefficients in the third row are given by:

$$
\beta_{n-1} = \frac{\phi_{n-1}\phi_{n-2} - \phi_n\phi_{n-3}}{\phi_{n-1}}
$$
$$
\beta_{n-3} = \frac{\phi_{n-1}\phi_{n-4} - \phi_n\phi_{n-5}}{\phi_{n-1}}
$$

etc.

The new coefficients in the fourth row are given in the same way:

$$
\xi_{n-1} = \frac{\beta_{n-1}\phi_{n-3} - \phi_{n-1}\beta_{n-3}}{\beta_{n-1}}
$$
$$
\xi_{n-3} = \frac{\beta_{n-1}\phi_{n-5} - \phi_{n-1}\beta_{n-5}}{\beta_{n-1}}
$$

The first necessary part of Theorem 2.5 will here be used for disproving the ability of moving the zeros into the left half-plane.

Theorem 2.5 says only if all the zeros are to the left of the imaginary axis or not. It would perhaps be more useful to set a performance criterion that the zeros should lie a certain distance (say ψ) into the left half-plane. This is certainly possible and the only thing which needs to be done is performing a coordinate transformation before applying theorem 2.5. That means you have to place the new coordinate system in such a way that $s = \psi$ in the original coordinate system must correspond to $s' = 0$ in the new system. Thus the coordinate transformation will take the form $s' = s - \psi$. See figure 2.2 for a graphical interpretation of the coordinate transformation.

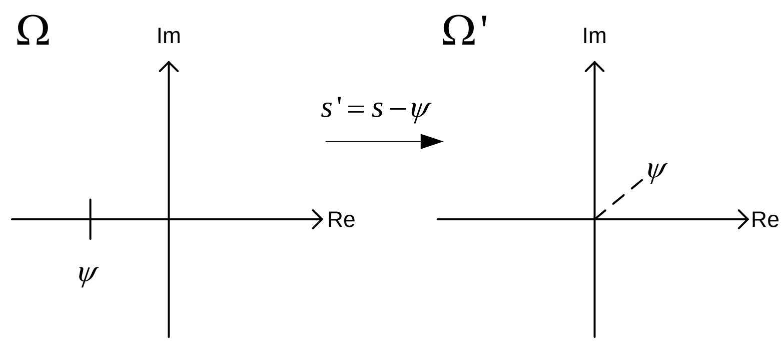

Figure 2.2

2.4 Bandwidth criterion

It is well-known from control theory that stabilizing a system with both unstable zero-and pole dynamics is very difficult. In [4] there is a set of controllability rules based on the plant dynamics only. There are two rules concerning RHP-zeros and RHP-poles.

Theorem 2.6 *For stabilizing an unstable plant we need high feedback gains, and thus there will be a certain requirement to the bandwidth.*

- $w_c > 2p$ *for a real unstable pole at s=p*
- $w_c > 0.67(x + \sqrt{4x^2 + 3y^2})$ *for a pair of unstable complex conjugated poles* $p = x \pm jy$
- $w_c > 1.15|p|$ *for a pair of purely imaginary poles* $p = j|p|$

Theorem 2.7 *Right half plane (RHP) zeros limit the bandwidth.*
Tight control at low frequencies with a RHP-zero z

- $w_c < z/2$ *for a real RHP-zero*
- $w_c < 0.86|z|$ *for an imaginary RHP-zero*

Theorem 2.6 can be verified if one thinks physically on controlling an unstable system. This control system must at least be fast enough to avoid the instability to develop. This means that the bandwidth must be at least greater than some value.

Theorem 2.7 can be supported by the fact that if one use a simple proportional controller, the open-loop system's zeros move to the closed-loop poles. In other words, if the open-loop has unstable zero dynamics, there is an upper limit for K which certainly limit the bandwidth.

Only real zeros will be investigated further. And the following theorem can be stated.

Theorem 2.8 *For performance at low frequencies with both unstable zero-and pole dynamics, the bandwidth must lie in the interval:*

- $2p{<}w_c{<}\frac{z}{2}$ *for a real unstable pole at* $s{=}p$
- $0.67(x+\sqrt{4x^2+3y^2}) < w_c < \frac{z}{2}$ *for a pair of unstable complex conjugated poles* $p = x \pm jy$

3 Example process

For problem concretization, it is here defined an example process with to measurements y_1 and y_2 defined in (3.1) and (3.2). By considering the closeness of the zero and the pole in y_1 and y_2 respectively, controlling either of them alone will be impossible in a practical sense. Designing a multivariable controller would be a possible approach. However, the question here is whether a more simple approach is viable (i.e. linear combination of measurements). The linear combination is defined in (3.3)

$$y_1 = 5 \underbrace{\frac{(-1,5s+1)}{-s+1}}_{G_1} u \tag{3.1}$$

$$y_2 = 5 \underbrace{\frac{-0.5s+1}{-s+1}}_{G_2} u \tag{3.2}$$

$$y = y_2 + \alpha y_1 \tag{3.3}$$

3.1 Controllability analysis

Applying theorem 2.8 for performance at low frequencies to the example process defined in (3.1) and (3.2) yields respectively:

$$\begin{aligned} z_{y1} &= 0.67, p_{y1} = 1 \\ 2 &< w_c < 0.335 \end{aligned}$$

and

$$\begin{aligned} z_{y2} &= 2, p_{y2} = 1 \\ 2 &< w_c < 1 \end{aligned}$$

where z_{yi} is the zero for y_i and p_{yi} is the pole for y_i.

When controlling only one loop, performance at low frequencies is certainly desirable. In this case, however, this is not possible as can be seen from the contradicting bandwidth interval of the two measurements y_1 and y_2.

In addition to these theorems, concluding remarks on performance limitations can be drawn from the waterbed formula given in theorem 2.1. Because of both unstable pole - and zero dynamics this will give an unwanted peak in the sensitivity function. The peaks of S, T and KS are calculated in table 3.1 based on the formulas given in theorem 2.2, 2.3 and 2.4.

	$G1$	$G2$
|S|	5	3
|T|	5	3
|KS|	0.8	0.8

Table 3.1: Bounds on peaks for some closed-loop transfer functions

From equation (2.1) it can be concluded that the closed-loop transfer functions S and T should be small to avoid amplifying disturbances and measurement noise. KS on the other hand is defined in equation (2.2), and says something about input-usage. If the transfer function is properly scaled, KS should be less than one for all frequencies to avoid input saturation. If the manipulated input saturates, it means that the control system is effectively open-loop. Saturation is then especially dangerous when controlling an open-loop unstable system. In this case $|KS|$ is less than 1, and it means that input-usage is not a problem.

Most of these comments above point out that controlling y_1 or y_2 alone will almost be impossible. This can also be verified if one tries to calculate the closed-loop poles using a proportional controller only. It is then easy to show that for the plant in (3.1) the controller gain K needs to be in the interval given in (3.4).

$$-0.200 < K < -0.133 \tag{3.4}$$

This interval is small due to the closeness of the unstable zero and pole dynamics. Stabilizing this plant is certainly hard, and even worse if you want to get an acceptable performance.

3.2 Model-uncertainty

Defining the linear combination $\alpha y_1 + y_2$ and the following transfer functions for the measurements:

$$y_1 = \frac{-bs + c}{-s + 1} u \tag{3.5}$$

$$y_2 = \frac{-ds + e}{-s + 1} u \tag{3.6}$$

This linear combination places the zero at:

$$s = \frac{\alpha c + e}{\alpha b + d} \tag{3.7}$$

If you want the zero to lie in the left half-plane the linear-combination parameter α must be chosen accordingly. It can be shown that the parameter α must lie in the following interval if $-\frac{d}{b} > -\frac{e}{c}$

$$-\frac{e}{c} < \alpha < -\frac{d}{b} \tag{3.8}$$

or if $-\frac{d}{b} < -\frac{e}{c}$

$$-\frac{d}{b} < \alpha < -\frac{e}{c} \tag{3.9}$$

In other words if $\frac{e}{c} = \frac{d}{b}$ it is impossible to move the zero into the left half-plane. What this equality actually means is that if you have two measurements with the same zero (but not necessary the same gain) it is impossible to move the zero of the linear combination into the left half-plane. Further says (3.8) and (3.9) that if the two measurements are very similar (similar zeros) you would get a very small interval to pick an α from. A smaller interval will mean that the system would be even more exposed to model uncertainty.

For the plant defined in (3.1) and (3.2) the parameter α must lie in the interval given in (3.10) if the zero of the linear combination of these two measurements is to lie in the left half-plane.

$$-1 < \alpha < -0.33 \tag{3.10}$$

The zero of the linear combination is also plotted as a function of the parameter α in figure 3.1.

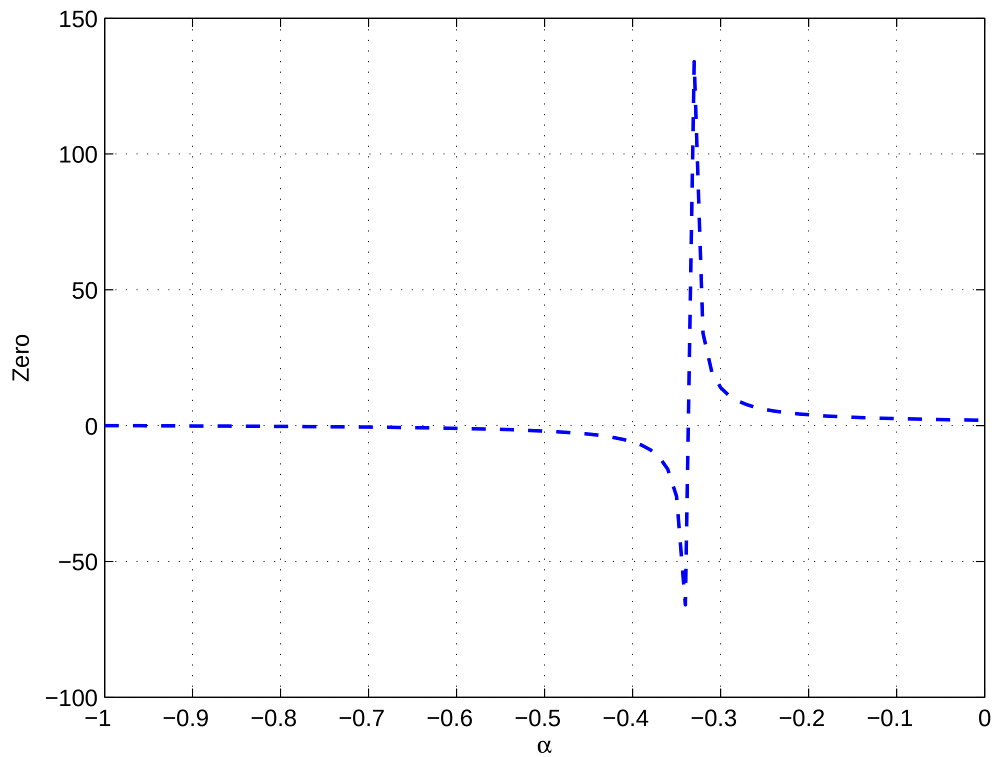

Figure 3.1: The movement of the zero of the linear combination as a function of α

The question that arises then is what value of α should be chosen? Certainly in the interval between -1 and -0.333. But the value should not be too close to -0.33 as can be seen from (3.7) since the pole goes to minus infinity. Even `Matlab` gets trouble with simulations when α gets greater than -0.4. Since the inner-loop is only designed for the purpose of stabilizing, the zero should only lie as far into the left half-plane as is necessary for robustness against model-uncertainty. Large gain of the linear combination is not necessary since it is used for stabilizing purpose only. Performance is not an issue for this inner loop.

3.3 Using theorem 2.5

By using theorem 2.5 it can be shown that it is possible to move the zeros into the left half plane by adjusting the linear combination parameter α. Using the linear combination $y = \alpha y_1 + y_2$ with y_1 and y_2 given in (3.5) and (3.6). This gives the following zero polynomial:

$$P_n(s) = \underbrace{(-7.5\alpha - 2.5)}_{>0} s + \underbrace{5\alpha + 5}_{>0} \tag{3.11}$$

which gives the following allowable interval for α

$$-1 < \alpha < -0.333 \tag{3.12}$$

Notice that requiring that both the constants in (3.11) are positive is in this case both a necessary and sufficient condition.

This interval is actually the same as was outlined in (3.10), but this method is much more applicable to more complex systems with several zeros.

This interval which is outlined here, tells us that it is possible to move the zeros into the left half-plane, but nothing more. A more interesting approach is to try to investigate if we can move the zero to left of some desired value. It is possible to use the method outlined in section 2.3 by first perform a coordinate transformation, and thereafter applying theorem 2.5.

A simple example can illustrate this fact. Let us set a performance criterion that all the zeros should lie to the left of $s = -1$. That means $\phi = -1$. The new zero polynomial will take the form:

$$P_n(s') = (s' - 1)(-2.5 - 7.5\alpha) + 5 + 5\alpha$$

$$P_n(s') = (-2,5 - 7.5\alpha)s' + 7.5 + 12.5\alpha \tag{3.13}$$

And the resulting interval to pick an α from is given below:

$$-0.6 < \alpha < -0.33 \tag{3.14}$$

This means that the linear combination parameter α must be chosen to lie in the interval between -0.6 and -0.33 if the zero is to lie to the left of $s = -1$.

3.4 Stabilizing the plant with cascade control

Consider the case where y_1 is the measurement we actually want to control, and y_2 is an extra measurement used for achieving the overall control objective. The idea is to control y_1 in a cascade manner, where a linear combination of y_1 and y_2 is used for stabilization in an inner loop. The outer control loop takes care of the set-point tracking for y_1. Figure 3.2 shows the control structure in a block diagram.

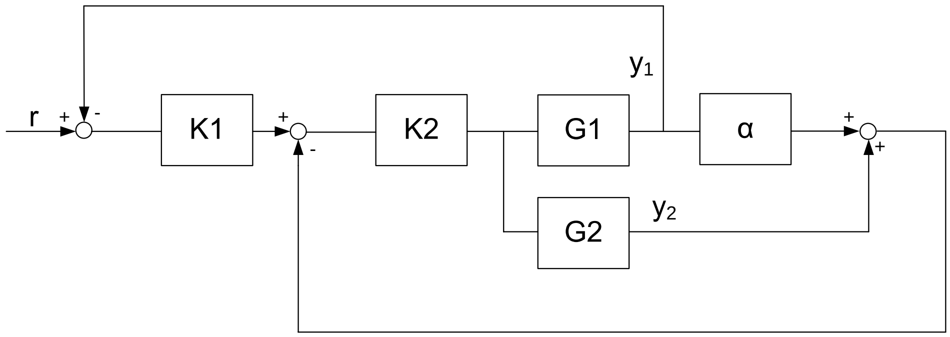

Figure 3.2

In this example the idea is to try to control y_1 with an acceptable performance. As commented in the controllability analysis of this simple example in section 3.1, it was concluded that controlling y_1 alone is hopeless because of the closeness of the unstable pole and zero. The idea is then to make use of another measurement (which in this case is y_2) and make use of this measurement in a linear combination with a measurement of y_1. The reason for this is to try to move the unstable zero into the left half-plane, because it is then easier to stabilize the system. After the system is stabilized, it is possible to wrap another feedback loop around to control y_1 in a cascade manner. When designing a cascade controller it is important to make sure that the inner loop is much faster than the outer loop. In other words, the inner control loop must have a greater bandwidth than the outer control loop.

When designing a cascade controller for this system it was only used a simple proportional controller for the inner stabilizing control loop. No set-point tracking is necessary for this inner loop because it is designed for only one purpose, namely stabilizing. Integral action in this inner loop would actually only make it worse to stabilize. Since the purpose is to control y_1 only, it is enough to include integral action in the outer control-loop.

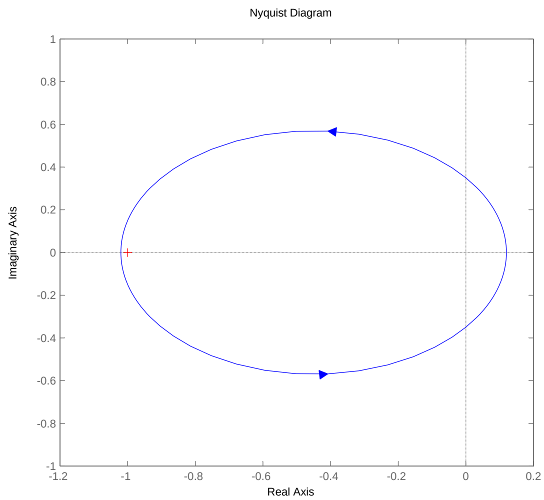

Figure 3.3

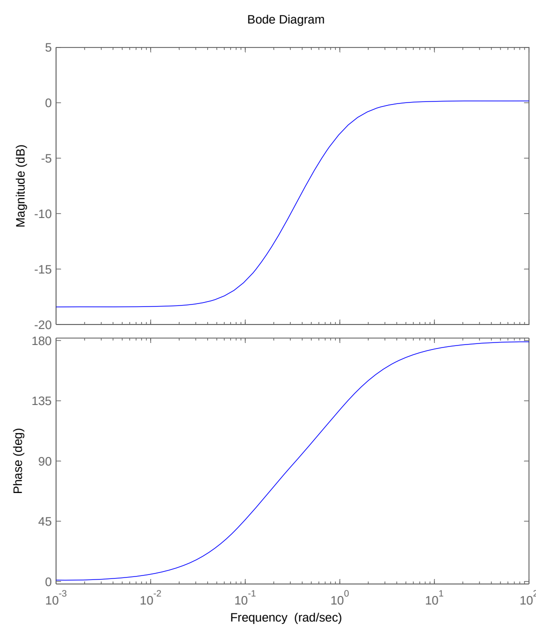

Figure 3.4

The controller design for the inner loop was based on the nyquist- and bode diagram given in figure 3.3 and 3.4. Since the linear combination system still has one right half-plane pole, the locus of the open-loop transfer function GK must encircle the critical point $(-1, 0)$ one time anticlockwise if the closed-loop is to be stable.

As can be seen from the nyquist diagram, the lower bound on the controller gain is $K = 0.24$. If the controller gain was less than this value, the critical point would be outside the locus of GK, and the closed-loop would become unstable.

The closed-loop from $\frac{y_1}{r}$:

$$\frac{y_1}{r} = \frac{G_1K_1K_2}{1 + G_2K_2 + G_1K_1K_2 + G_1K_2\alpha} \tag{3.15}$$

The closed-loop transfer function $\frac{y_1}{r}$ given in equation (3.15) indicates that any potential right half-plane zeros in G_1 will still be a limitation in the closed-loop transfer function. This is somewhat interesting. The zero of the linear combination is changed and it is no longer a fundamental controllability limitation for the inner loop. However y_1 will still be limited by inverse response. This means that the outer loop has an upper limitation in bandwidth, because of this RHP-zero. This could be a limitation if we want fast control in the outer loop.

3.5 Simulations of process example

Simulations are done with a unit-step change in the reference signal at t=10. See figure 3.5. The control structure is given in figure 3.2. Notice that the linear combination is NOT exposed to inverse response. However y_1, which is controlled in an outer loop, is still limited with inverse response. Note that the responses are somewhat unphysical. This is because the two transfer functions defined in equation (3.1) and (3.2) are semi-proper, and will amplify for fast frequencies.

The following controllers were used corresponding to figure 3.2.

$$K_2 = 20 \tag{3.16}$$

$$K_1 = K_{ytre}(1 + \frac{1}{T_i s}) = 0.1(1 + \frac{1}{10s}) \tag{3.17}$$

$$\alpha = -0.9 \tag{3.18}$$

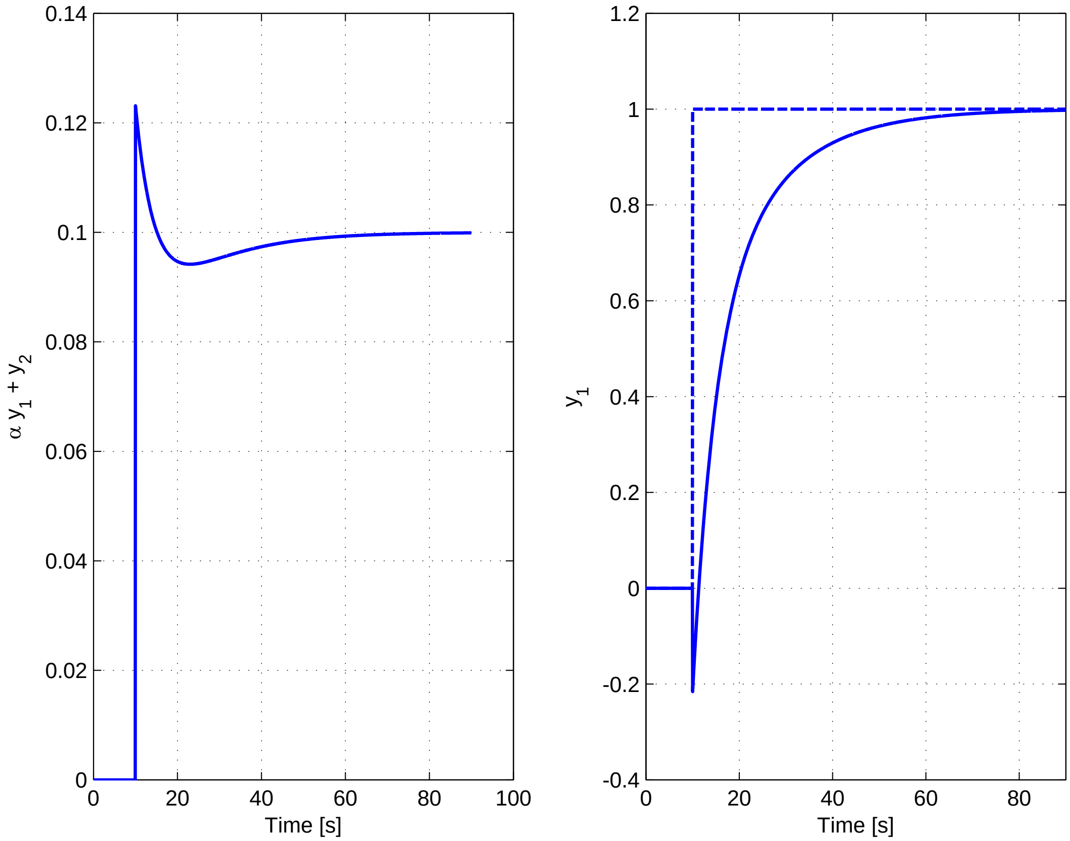

Figure 3.5: Time response for the inner and outer-loop with a unit-step change in the reference

4 Slugging example

The linear combination approach was shown to work well for the example process in section 3. The example process, however, has much simpler dynamics than most of the slugging related topside measurements. It will here be defined transfer functions from the choke-valve opening z to several topside-measurements. First it will be performed a controllability analysis of these transfer functions, before it is proposed a linear combination of them for the purpose of stabilization. But first of all a short description of how these transfer functions are developed will be given.

4.1 Linearization of a simplified two-phase flow model

The model which is used here is developed in [5] and is restated in appendix A. A `Simulink` implementation of this model developed by [5] was used as a basis for linearization. This was done instead of trying to linearize the system in appendix A analytical. The linearization was performed by designing a controller which stabilized the system at a desired choke-valve opening for the `Simulink` model. This was done because it is then easy to find the unstable stationary point. The linearization was performed around the choke-valve openings of 17.5% and 30%, and transfer functions were found between the disturbances $w_{G,in}$, $w_{L,in}$ and P_0 in addition to the manipulated variable z to several measurements. These transfer functions can be found in appendix B.

4.2 Transfer functions from z to the measurements

The transfer functions which will be analyzed further are restated here. These are the transfer functions between the manipulated variable z and the measurements.

$$DP = -4.45\frac{(0.9020s-1)(83.51s-1)}{(0.494s+1)(9009s^2-71.8s+1)}z \tag{4.1}$$

$$\rho_T = -14.73\frac{(253.5s-1)(2321s+1)}{(0.494s+1)(9009s^2-71.8s+1)}z \tag{4.2}$$

$$W = -1.03\cdot 10^{-7}\frac{(0.393s+1)(2681s+1)(1.02\cdot 10^{10}s-1)}{(0.494s+1)(9009s^2-71.8s+1)}z \tag{4.3}$$

$$\alpha_{LM} = -2.85\cdot 10^{-10}\frac{(273.48s-1)(2.94\cdot 10^{10}s+1)}{(0.494s+1)(9009s^2-71.8s+1)}z \tag{4.4}$$

$$\alpha_{LT} = -0.0188\frac{(255.71s-1)(2642s+1)}{(0.494s+1)(9009s^2-71.8s+1)}z \tag{4.5}$$

$$Q = 4.59\cdot 10^{-4}\frac{(0.688s+1)(353.1s+1)(2227s+1)}{(0.494s+1)(9009s^2-71.8s+1)}z \tag{4.6}$$

4.3 Controllability analysis

The poles of the system are given in below. The poles of the system are obviously observable through all of the measurements given in (4.1)-(4.6).

$$p_1 = -2.0247$$
$$p_2 = 0.0040 + 0.0098i$$
$$p_3 = 0.0040 - 0.0098i$$

For a system with a pair of complex RHP-poles $p = x \pm jy$ we require a bandwidth according to theorem 2.6:

$$w_c > 0.0153 \tag{4.7}$$

Because of the complex conjugated pair of poles, there is a lower bound on the bandwidth which must på achieved. This is because the control system must be able to react fast enough to avoid the instability to develop. The question is then if the RHP-zeros in the measurement transfer functions given in (4.1)-(4.6) will give a consistent interval as defined in theorem 2.8

4.3.1 Controllability of y=DP

From equation (4.1) it can be seen that the measurement has a high steady-state gain ($|DP(0) = 4.45|$) which is good for tight control at low frequencies. With a low steady-state gain it would be problematic to keep the controlled variable at the set-point. The system would drift away.

It is then necessary to investigate the system with respect to the closeness of the RHP-zeros and the RHP complex conjugated poles. The transfer function between the measurement of DP and the choke valve z, which is given in (4.1), has two RHP-zeros. The worst zero (that means the zero closest to the origin) gives the following upper bound on the bandwidth according to theorem 2.7.

$$w_c < 0.0060 \tag{4.8}$$

which together with (4.7) give an unattainable interval for the bandwidth.

In addition to this, it can be seen from the nyquist diagram how hopeless it actually is to stabilize the system (see figure 4.1). For stabilizing the system in closed-loop, the locus of the open loop GK must encircle the critical point two times anticlockwise. When analyzing stability for open-loop unstable system, one has to be very careful when using bode diagram for concluding if the closed-loop is stable. However, one can use the nyquist plot and see how it corresponds to the bode diagram. And after this comparison, conclusions can be made from the bode diagram.
For closed-loop stability there are two requirements that can be drawn from the nyquist and bode diagram. The first is a requirement to the steady-state gain. This has to be lower than 1, which in the bode-diagram means that the amplitude must be lower than 0-dB at steady-state. The second requirement is that the amplitude has to be greater than 1 when the phase hits 180 degrees for the second time. This is very hard to see from the bode-diagram, but the phase starts at 180 degrees, before it's decreasing a bit, before it again turns and hits 180 degrees.

Figure 4.1 is an open-loop plot of $k * DP$ where k is a simple proportional controller. The nyquist diagram is plotted for $k = 0.1$, $k = 0.2$ and $k = 0.3$. The only k which gives a stable closed-loop is $k = 0.2$. This interval is certainly not very large, and indicates that stabilizing DP in a single loop is hopeless in a practical sense.

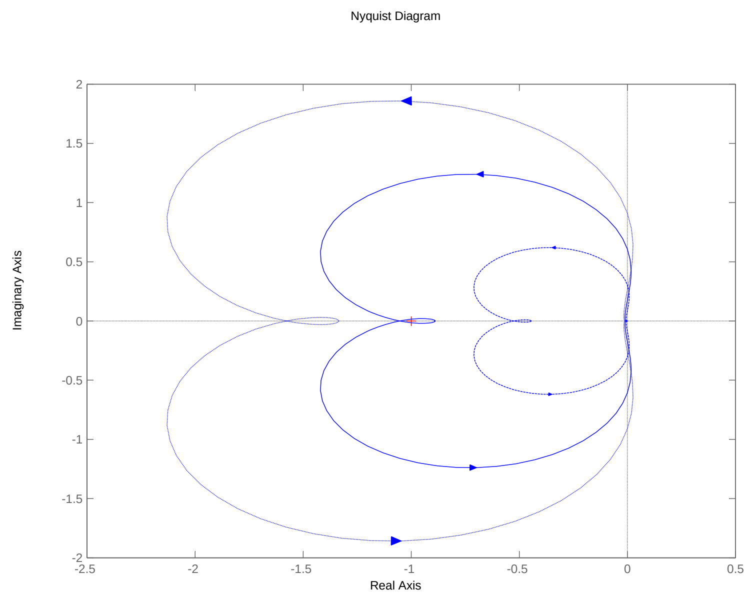

Figure 4.1

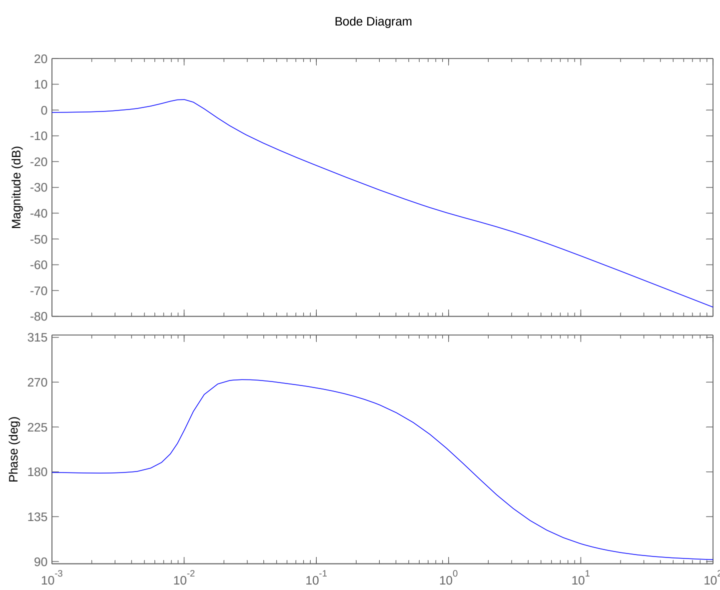

Figure 4.2

4.3.2 Controllability of y=ρ_T

Equation (4.2) defines the transfer function from z to ρ_T. $|\rho_T(0)| = 14.73$ which is a high steady state gain indicating that drifting will not be a problem.

However there is one RHP-zero. By using theorem 2.7 for performance at low frequencies the lower bound on the achievable bandwidth is

$$w_c < 0.0020 \tag{4.9}$$

which together with (4.7) gives an unattainable interval for the bandwidth. Figure 4.3 shows the nyquist diagram for the open-loop with at proportional controller. The nyquist plot shows that it is impossible to stabilize this process with any proportional controller.

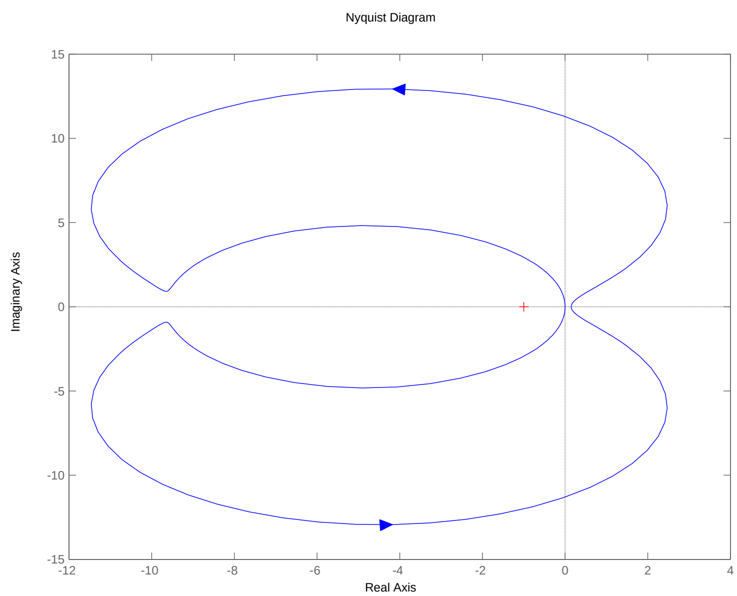

Figure 4.3

4.3.3 Controllability of y=W

Using $y = W$ as the controlled variable in a SISO-loop would be problematic because of the extremely low steady-state gain ($|W(0)| = -1.03 \cdot 10^{-7}$). In addition to this will the RHP-zero close to the imaginary axis be a problem for performance and give a very low bound on the bandwidth. This bound will according to theorem 2.7 be

$$w_c < 4.90 \cdot 10^{-11} \tag{4.10}$$

which together with (4.7) give an unattainable interval for the bandwidth.

4.3.4 Controllability of $y = \alpha_{LM}$

As with the measurement of $y = W$, $y = \alpha_{LM}$ has a very low steady-state gain which will cause drifting and bad performance $|\alpha_{LM}| = -2.85 \cdot 10^{-10}$. In addition to this the RHP-zero will cause a bandwidth limitation according to theorem 2.7 be:

$$w_c < 0.00183 \tag{4.11}$$

which together with (4.7) give an unattainable interval for the bandwidth.

4.3.5 Controllability of $y = \alpha_{LT}$

The transfer function from z to α_{LT} also has a low steady-state gain ($|\alpha_{LT}| = 0.0188$) which would cause drifting. In addition to this the RHP-zero will cause a bandwidth limitation according to theorem 2.7 :

$$w_c < 0.0020 \tag{4.12}$$

which together with (4.7) give an unattainable interval for the bandwidth.

4.3.6 Controllability of y=Q

The problem with using $y = Q$ as a controlled variable in a SISO loop is its low steady-state gain, which would cause drifting ($|Q(0)| = 4.59 \cdot 10^{-4}$). However, the transfer function from z to $y = Q$ does not contain any RHP zeros which cause any fundamental control performance limitations. Therefore $y = Q$ has been tried using as a stabilizing inner loop, using another measurement in an outer loop for performance. This approach has been taken by [3].

4.4 Linear combinations

In section 4.3 the focus was on controllability of various measurements in a SISO-loop. This controllability analysis was done for showing how hopeless it is to use only a single loop for stabilizing slug flow when considering topside measurements only. Now the idea is to use the linear combination approach in the same way as with the example process in section 3. It will here be focused on three linear combinations of measurements. DP and ρ_T, DP and W, ρ_T and W.

4.4.1 Linear combination of measurements - DP and ρ_T

Considering the linear combination $y = \rho_T + \alpha_{DP}$. Theorem 2.5 is used for trying to find out if it is possible to move all the right half-plane zeros into the left half-plane. Below is the resulting zero polynomial.

$$P_z(\alpha, s) = \underbrace{(-8670000 - 335\alpha)}_{>0} s^2 + \underbrace{(30500 + 368\alpha)}_{>0} s + \underbrace{14.73 - 4.45\alpha}_{>0} \tag{4.13}$$

Theorem 2.5 says that a necessary condition for ensuring that the zeros of this polynomial are all to the left of the imaginary axis is that all the constants must have the same sign, as shown in equation (4.13).

$$\begin{aligned} \alpha &< -25880 \\ \alpha &> -82.88 \\ \alpha &< 3.31 \end{aligned}$$

The α must be chosen in such a way that these constants have the same sign. As can be seen above, there are contradicting requirements for the linear combination parameter α, which means that it is not possible to move all the zeros into the left half-plane.

4.4.2 Linear combination of measurements - DP and W

Considering the linear combination $y = W + \alpha DP$. Theorem 2.5 is used for trying to find out if it is possible to move all the right half-plane zeros into the left half-plane. Below is the resulting zero polynomial.

$$P_z(\alpha, s) = \underbrace{1.102 \cdot 10^6}_{\phi_3} s^3 + \underbrace{(2.805 \cdot 10^6 + 335.1\alpha)}_{\phi_2} s^2 + \underbrace{(1046 - 375.6\alpha)}_{\phi_1} s + \underbrace{4.45\alpha}_{\phi_0} \tag{4.14}$$

$$\begin{aligned} 1.102 \cdot 10^6 &> 0 \\ \alpha &> -8370.6 \\ \alpha &< 2.78 \\ \alpha &> 0 \end{aligned}$$

$$0 < \alpha < 2.78 \tag{4.15}$$

Based on the equations above, using a linear combination with these two measurements looks promising. To prove that it is actually possible to move the zeros, one would need to apply the rest of Routh's criterion. In this case, this means that the following parameters defined under should have the same sign as the parameters in the root-polynomial. (which in this case means positive).

$$\beta_2 = \frac{\phi_2\phi_1 - \phi_3\phi_0}{\phi_2} = \frac{-1.259 \cdot 10^5 a^2 - 1.054 \cdot 10^9 a + 2.934 \cdot 10^9}{2.805 \cdot 10^6 + 335.1\alpha} \tag{4.16}$$

$$\delta_2 = \frac{\beta_2\phi_0}{\beta_2} = \phi_0 \tag{4.17}$$

Equation (4.17) does not impose any extra requirements. However, the polynomial given in (4.16) might. Having equation (4.15) in mind it is only necessary to investigate (4.16) for α's in this interval

$$-8413 < \alpha < 2.77 \tag{4.18}$$

which together with equation (4.15) give the following allowable interval for α:

$$0 < \alpha < 2.77 \tag{4.19}$$

Simulations were done using the control structure given in figure 3.2 where $G_1 = DP$ and $G_2 = W$. The differential pressure DP is used in the outer cascade. Below is the specification of the controller gains and integral time used in the simulations.

$$K_2 = 10 \tag{4.20}$$

$$K_1 = K_{ytre}(1 + \frac{1}{T_i s}) = 0.01(1 + \frac{1}{100s}) \tag{4.21}$$

$$\alpha = 1.0 \tag{4.22}$$

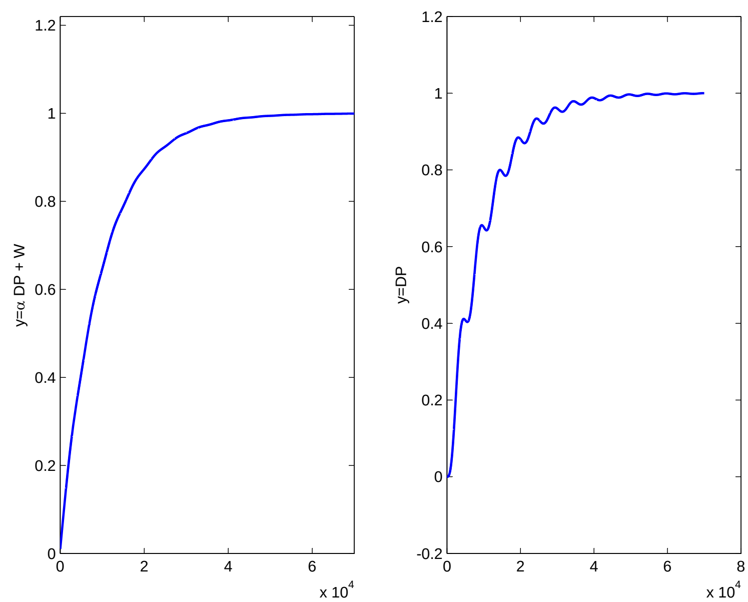

Figure 4.4: Response to a unit step in the reference for $y = DP$

To the left in figure 4.4 the response to a unit step in the reference of DP of the linear combination is shown. To the right the response of $y = DP$ is shown.

4.4.3 Linear combination of measurements - ρ_T and W

Considering the linear combination $y = W + \alpha\rho_T$. Theorem 2.5 is used for trying to find out if it is possible to move all the right half-plane zeros into the left half-plane. Below is the resulting zero polynomial.

$$P_z(\alpha, s) = 1.102 \cdot 10^6 s^3 + (8.67 \cdot 10^6\alpha + 2.805 \cdot 10^6)s^2 + (-3.05 \cdot 10^4\alpha + 1046)s - 14.73\alpha \tag{4.23}$$

$$\begin{aligned} 1.102 \cdot 10^6 &> 0 \\ \alpha &> -0.324 \\ \alpha &< 0.034 \\ \alpha &< 0 \end{aligned}$$

which give the following interval for α

$$-0.324 < \alpha < 0 \tag{4.24}$$

Based on the equations above, using a linear combination with these two measurements looks promising. To prove that it is actually possible to move the zeros, one would need to apply the rest of Routh's criterion. In this case, this means that the following parameters defined under should have the same sign as the parameters in the root-polynomial. (which in this case means positive).

$$\beta_2 = \frac{\phi_2\phi_1 - \phi_3\phi_0}{\phi_2} = \frac{-2.644 \cdot 10^4 a^2 - 7.64 \cdot 10^1 0\alpha + 2.934 \cdot 10^9}{8.67 \cdot 10^6\alpha + 2.805 \cdot 10^6} \tag{4.25}$$

$$\delta_2 = \frac{\beta_2\phi_0}{\beta_2} = \phi_0 \tag{4.26}$$

It can be shown that neither equation (4.25) nor equation (4.26) does impose any extra requirements on α. This means that the interval already found in equation (4.24) is an interval for the linear combination parameter (α) which is able to move the zero of the linear combination into the left half-plane.

Simulations were done only with the linear combination of these two measurements (without the outer cascade).

$$K_2 = 5 \tag{4.27}$$

$$\alpha = -0.2 \tag{4.28}$$

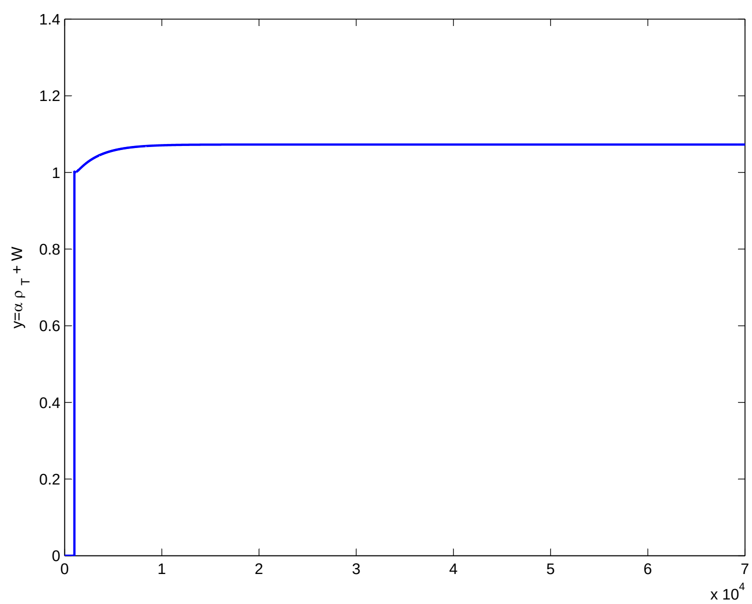

Figure 4.5: Response to a unit step in the reference for $y = \alpha + \rho_T W$

4.4.4 Comments on the choice of linear combinations

The idea was to use linear combinations which had right half-plane zeros. Therefore linear combinations with a measurement of the volume flow Q are not considered. Neither are linear combinations with α_{LM} and α_{LT} (See notation in appendix A.5). The reason for this is that they are so similar to the measurement of ρ_T. α_{LM} is the liquid fraction upstream the valve (mass basis) and α_{LT} is the liquid fraction upstream the valve (volume basis). ρ_T on the other hand, is the density upstream the valve. Since the density of the liquid is so dominating compared to the density of the gas, these measurements measure qualitatively the same.

4.4.5 Comments on the simulations

There were done some simulations on the two linear combination approaches which were able to move all the zeros into the left half-plane. However, these simulations were only done on the linear model of the plant, because applying these control structures to the non-linear plant seemed to fail.

5 Discussion and concluding remarks

Using topside measurements for diminishing riser-induced slug flow is wanted from an economic perspective to avoid installing new subsea equipment. However, most of these measurements are performance limited due to unstable zero dynamics.

Example process

The limitations using topside measurements were in this report first addressed using a simple process example with two measurements. These measurements contained one RHP-zero each. Using any of these measurements in a single loop and at the same time get an acceptable performance was shown to be impossible in a practical sense.

Therefore an approach using a linear combination of these to measurements to move the zero into the left half-plane was tried. This worked fine for the example process. However, such a linear combination was shown to be exposed to model-uncertainty. If the measurements were very similar in their placements of zeros, the exposure of model-uncertainty would even worsen.

It was also shown that even though it was possible to move the zero of the linear combination into the left half-plane, the outer feedback loop would still contain a RHP-zero. This could be a limitation if fast control is needed in the outer loop.

Slugging example

These problems would also come in to play for the more complex dynamic occurring from models of slug flow. But another problem occurred when the transfer functions had several zeros. A linear combination of these more complex transfer functions could fail to move the zeros of the linear combination into the left half-plane. Only two of three proposed linear combinations were shown to move all the zeros into the left half-plane. And the two linear combination that did, consisted of the measurement W where the RHP-zero almost lay at the origin.

It was here only confirmed if one was able to move the zeros into the left half-plane. This was done because it is then easy to conclude that there are no longer any limitations because of RHP-zeros. But the actual problem exists when the RHP-pole and RHP-zero are very close. There could very well be a possible approach to try to move the zeros in such a way that the criterion would be to ensure that the zeros were a certain distance from the pole (on either side of the RHP-pole). But to give a general performance criterion and a way to make sure that a good solution to the problem exists, would be much more difficult. And given that one is exposed to model-uncertainty, the work trying to find such a solution would perhaps be useless, because it would perhaps not work on the real system.

Comments to simulations on the non-linear plant

Applying the linear combination controller for the slugging example to the non-linear model did not seem to work. It can certainly well be that such a controller based on linear combination is not robust enough for coping with the non-linear plant. However, it should be mentioned that the implementation of this plant unfortunately can not be said to be fault free.

A Model Equations

A.1 Conservation equations

$$\frac{d}{dt}m_L = w_{L,in} - w_{L,out} \tag{A.1}$$

$$\frac{d}{dt}m_{G1} = w_{G,in} - w_{G1} \tag{A.2}$$

$$\frac{d}{dt}m_{G2} = w_{G1} - w_{G,out} \tag{A.3}$$

A.2 Calculation of state-dependent internal variables

$$P_1 = \frac{m_{G1}RT}{V_{G1}M_G} \tag{A.4}$$

$$\rho_{G1} = \frac{m_{G1}}{V_{G1}} \tag{A.5}$$

$$V_L = \frac{m_L}{\rho_L} \tag{A.6}$$

$$h_1 A_1 + V_{LR} = V_L \tag{A.7}$$

$$V_T = A_2(H_2 + L_3) \tag{A.8}$$

$$V_{G2} = V_T - V_{LR} \tag{A.9}$$

$$\rho_{G2} = \frac{m_{G2}}{V_{G2}} \tag{A.10}$$

$$\alpha_L = \frac{V_{LR}}{V_T} \tag{A.11}$$

$$P_2 = \frac{m_{G2}RT}{V_{G2}M_G} \tag{A.12}$$

$$\bar{\rho} = \frac{m_{G2} + V_{LR}\rho_L}{V_T} \tag{A.13}$$

$$\bar{\rho}g(H_2 + H_3) - \rho_L g h_1 = P_1 - P_2 \tag{A.14}$$

$$\alpha_{LT} = (V_{LR} > H_2A_2)\alpha^*_{LT} + \frac{w^n}{1+w^n}(\alpha_L - (V_{LR} > H_2A_2)\alpha^*_{LT}) \tag{A.15}$$

$$\alpha^*_{LT} = \frac{V_{LR} - A_2H_2}{A_2L_3} \tag{A.16}$$

$$w = \frac{K_3\rho_{G1}v_{G1}^2}{\rho_L - \rho_{G1}} \tag{A.17}$$

$$\rho_T = \alpha_{LT}\rho_L + (1-\alpha_{LT})\rho_{G2} \tag{A.18}$$

$$\alpha_L^m = \frac{\alpha_{LT}\rho_L}{\alpha_{LT}\rho_L + (1-\alpha_{LT})\rho_{G2}} \tag{A.19}$$

A.3 Flow equations

$$v_{G1} = (h_1 < H_1) K_2 \frac{H_1 - h_1}{H_1} \sqrt{\frac{P_1 - P_2 - \rho_L g \alpha_L H_2}{\rho_{G1}}} \tag{A.20}$$

$$w_{G1} = v_{G1} \rho_{G1} \hat{A} \tag{A.21}$$

$$m_{mix,out} = K_1 z \sqrt{\rho_T (P_2 - P_0)} \tag{A.22}$$

$$w_{G,out} = (1 - \alpha_L^m) m_{mix,out} \tag{A.23}$$

$$w_{L,out} = \alpha_L^m m_{mix,out} \tag{A.24}$$

A.4 Geometric equations

$$H_1 = \frac{2r}{cos(\theta)} \tag{A.25}$$

$$A_1 = \frac{A_2}{sin(\theta)} \tag{A.26}$$

$$\phi = \left(\pi - acos \left(1 - \frac{(H_1 - h_1) cos(\theta}{r} \right) \right) \tag{A.27}$$

$$\hat{A} = r^2 (\pi - \phi - cos(\pi - \phi) sin(\pi - \phi)) \tag{A.28}$$

A.5 Notation

Symbol	Description	Unit	Remarks
m_{Gi}	Mass of gas in volume i	Kg	State variable
m_L	Mass of liquid	Kg	State variable
V_{Gi}	Gas volume i	m^3	$V_{G1} = const$
V_L	Volume occupied by liquid	m^3	
V_{LR}	Volume of liquid in riser	m^3	
V_T	Total volume in riser	m^3	
P_i	Pressure in volume i	$\frac{N}{M^2}$	
ρ_{Gi}	Gas density in volume i	$\frac{kg}{m^3}$	
ρ_L	Liquid density	$\frac{kg}{m^3}$	Constant
$\bar{\rho}$	Average density in riser	$\frac{kg}{m^3}$	
ρ_T	Density upstream valve	$\frac{kg}{m^3}$	
v_{G1}	Gas velocity at lowpoint	$\frac{m}{s}$	
$v_{mix,out}$	Liquid velocity through choke valve	$\frac{m}{s}$	
w_{G1}	Internal gas mass flowrate	$\frac{Kg}{s}$	
$w_{G,out}$	Gas mass flowrate through choke valve	$\frac{Kg}{s}$	
$w_{L,out}$	Liq.mass flowrate through choke valve	$\frac{Kg}{s}$	
α_L	Average liq. frac. in riser, volume basis	-	
α_{LT}	Liq. frac. upstream valve, volume basis	-	
α_L^m	Liq. frac. upstream valve, mass basis	-	
α_{LT}^*	Liq. frac. upstream valve, without entr.	-	
h_1	Liquid level upstream the dip	m	
H_1	Critical liquid level	m	Constant
H_2	Height of riser	m	Constant
r	Radius of pipe	m	Constant
A_1	Area in the horizontal plane, V_1	m^2	Constant
A_2	Cross section area, V_2	m^2	Constant
$\hat{A}$	Gas flow area at lowpoint	m^2	
L_3	Length of horizontal top section	m	Constant
θ	Feed pipe inclination	rad	Constant
R	Gas constant	$8314 \frac{J}{K \cdot Kmol}$	Constant
g	Spesific gravity	$9.81 \frac{m}{s^2}$	Constant
T	System temperature	K	Constant
M_G	Molecular weight of gas	$\frac{Kg}{Kmol}$	Constant
$w_{G,in}$	Mass rate of gas into system	$\frac{Kg}{s}$	Disturbance
$w_{L,in}$	Mass rate of liquid into system	$\frac{Kg}{s}$	Disturbance
P_0	Pressure after choke valve	$\frac{N}{M^2}$	Disturbance
z	Valve position	-	Input
K_1	Choke valve constant	-	Tuning parameter
K_2	Gas flow constant	-	Tuning parameter
K_3	Friction parameter	-	Tuning parameter
n	w^n in the friction expression	-	Tuning parameter

Table A.1: Notation

B Transfer functions

Transfer functions when $z = 30\%$

Obtained from Espen Storkaas 3-state model for two-phase flow. [5]
The transfer functions are not scale.

Manipulated variable z and disturbance $w_{G,in}$		
	z	$w_{G,in}$
P_1	$-4.74\frac{(324s+1)}{(0.494s+1)(9002s^2-71.8s+1)}$	$-23.95\frac{(0.513s+1)(21.79s-1)}{(0.494s+1)(9002s^2-71.8s+1)}$
DP	$-4.45\frac{(0.9020s-1)(83.51s-1)}{(0.494s+1)(9002s^2-71.8s+1)}$	$0.6494\frac{(0.480s+1)(786.4s+1)}{(0.494s+1)(9002s^2-71.8s+1)}$
ρ_T	$-14.73\frac{(253.5s-1)(2321s+1)}{(0.494s+1)(9002s^2-71.8s+1)}$	$-401.59\frac{(1.524s-1)(278.8s+1)}{(0.494s+1)(9002s^2-71.8s+1)}$
W	$-1.03 \cdot 10^{-7}\frac{(1.02 \cdot 10^{10}s-1)(2681s+1)(0.393s+1)}{(0.494s+1)(9002s^2-71.8s+1)}$	$1.00\frac{(0.705s+1)(4364s+1)}{(0.494s+1)(9002s^2-71.8s+1)}$
Q	$4.59 \cdot 10^{-4}\frac{(0.688s+1)(353.1s+1)(2227s+1)}{(0.494s+1)(9002s^2-71.8s+1)}$	$0.014\frac{(0.0876s+1)(323.6s+1)}{(0.494s+1)(9002s^2-71.8s+1)}$
α_{LM}	$-2.85 \cdot 10^{-10}\frac{(273.48s-1)(2.94 \cdot 10^{10}s+1)}{(0.494s+1)(9002s^2-71.8s+1)}$	$-0.1066\frac{(273.14s-1)(1.54s+1)}{(0.494s+1)(9002s^2-71.8s+1)}$
α_{LT}	$-0.0188\frac{(255.71s-1)(2642s+1)}{(0.494s+1)(9002s^2-71.8s+1)}$	$-0.5903\frac{(278.06s-1)(1.526s+1)}{(0.494s+1)(9002s^2-71.8s+1)}$

Table B.1: Linearized around a choke-valve of 30 %

Disturbances $w_{L,in}$ and P_0		
	$w_{L,in}$	P_0
P_1	$0.6970\frac{(53.96s+1)}{(0.494s+1)(9002s^2-71.8s+1)}$	$1.0613 \cdot 10^{-5}\frac{(3.44 \cdot 10^{-9}s+1)(324.4s+1)}{(0.494s+1)(9002s^2-71.8s+1)}$
DP	$0.1273\frac{(0.041s-1)(185.5s-1)}{(0.494s+1)(9002s^2-71.8s+1)}$	$-4.070 \cdot 10^{-8}\frac{(0.500s+1)(1081s+1)(1983s+1)}{(0.494s+1)(9002s^2-71.8s+1)}$
ρ_T	$17.34\frac{(65.29s+1)(188.7s-1)}{(0.494s+1)(9002s^2-71.8s+1)}$	$3.30 \cdot 10^{-5}\frac{(253.5s+1)(2321s+1)}{(0.494s+1)(9002s^2-71.8s+1)}$
W	$1.00\frac{(9.509s+1)(185.8s-1)}{(0.494s+1)(9002s^2-71.8s+1)}$	$6.11 \cdot 10^{-10}\frac{(3.40 \cdot 10^{6}s-1)(2679s+1)(0.393s+1)}{(0.494s+1)(9002s^2-71.8s+1)}$
Q	$0.0013\frac{(13.55s-1)(185.0s-1)}{(0.494s+1)(9002s^2-71.8s+1)}$	$-1.023 \cdot 10^{-9}\frac{(0.688s+1)(353.3s+1)(2220s+1)}{(0.494s+1)(9002s^2-71.8s+1)}$
α_{LM}	$0.0045\frac{(187.12s-1)(66.91s+1)}{(0.494s+1)(9002s^2-71.8s+1)}$	$2.37 \cdot 10^{-12}\frac{(273.47s-1)(7.92 \cdot 10^{6}s+1)}{(0.494s+1)(9002s^2-71.8s+1)}$
α_{LT}	$0.025\frac{(187.10s-1)(65.50s+1)}{(0.494s+1)(9002s^2-71.8s+1)}$	$4.22 \cdot 10^{-8}\frac{(255.71s-1)(2641s+1)}{(0.494s+1)(9002s^2-71.8s+1)}$

Table B.2: Linearized around a choke-valve of 30 %

Transfer functions when $z = 17.5\%$

Obtained from Espen Storkaas 3-state model for two-phase flow. [5]
The transfer functions are not scale.

Manipulated variable z and disturbance $w_{G,in}$		
	z	$w_{G,in}$
P_1	$23.47\frac{(326.6s+1)}{(0.508*s+1)(25504s^2-38.96s+1)}$	$-22.27\frac{(0.533s+1)(65.58s-1)}{(0.508*s+1)(25504s^2-38.96s+1)}$
DP	$-22.07\frac{(0.994s-1)(74.55s-1)}{(0.508*s+1)(25504s^2-38.96s+1)}$	$1.85\frac{(0.491s+1)(787.96s+1)}{(0.508s+1)(25504s^2-38.96s+1)}$
ρ_T	$70.609\frac{(252.9s-1)(2374s-1)}{(0.508*s+1)(25504s^2-38.96s+1)}$	$-392.95\frac{(4.151s+1)(288.6s-1)}{(0.508s+1)(25504s^2-38.96s+1)}$
W	$3.842 \cdot 10^{-7}\frac{(0.401s+1)(2677s+1)(2.51\cdot 10^{9}s-1)}{(0.508*s+1)(25504s^2-38.96s+1)}$	$1.00\frac{(1.296s+1)(4290s+1)}{(0.508s+1)(25504s^2-38.96s+1)}$
Q	$0.0022\frac{(0.699s+1)(354.0s+1)(2294s-1)}{(0.508*s+1)(25504s^2-38.96s+1)}$	$0.0139\frac{(0.927s-1)(324.16s+1)}{(0.508s+1)(25504s^2-38.96s+1)}$
α_{LM}	$-1.49 \cdot 10^{-9}\frac{(273.3s-1)(2.79\cdot 10^{10}s+1)}{(0.508*s+1)(25504s^2-38.96s+1)}$	$-0.107\frac{(272.9s-1)(4.31s+1)}{(0.508*s+1)(25504s^2-38.96s+1)}$
α_{LT}	$-0.090\frac{(255.2s-1)(2707s+1)}{(0.508s+1)(25504s^2-38.96s+1)}$	$-0.580\frac{(286.54s-1)(4.17s+1)}{(0.508s+1)(25504s^2-38.96s+1)}$

Table B.3: Linearized around a choke-valve of 17.5 %

Manipulated variable z and disturbance $w_{L,in}$		
	$w_{L,in}$	P_0
P_1	$-0.947\frac{(116.23s+1)}{(0.508*s+1)(25504s^2-38.96s+1)}$	$1.05 \cdot 10^{-5}\frac{(326.60s+1)}{(0.508*s+1)(25504s^2-38.96s+1)}$
DP	$0.370\frac{(0.0439s+1)(174.3s+1)}{(0.508*s+1)(25504s^2-38.96s+1)}$	$-1.15 \cdot 10^{-7}\frac{(0.510s+1)(1054s+1)(2095s+1)}{(0.508s+1)(25504s^2-38.96s+1)}$
ρ_T	$17.89\frac{(182.93s+1)(185.72s-1)}{(0.508*s+1)(25504s^2-38.96s+1)}$	$3.16 \cdot 10^{-5}\frac{(252.87s+1)(2374s+1)}{(0.508s+1)(25504s^2-38.96s+1)}$
W	$1.00\frac{(28.46s+1)(177.3s-1)}{(0.508*s+1)(25504s^2-38.96s+1)}$	$-1.03 \cdot 10^{-9}\frac{(0.401s+1)(2705s+1)(2.65\cdot 10^{5}s+1)}{(0.508s+1)(25504s^2-38.96s+1)}$
Q	$0.0013\frac{(42.93s-1)(167.68s-1)}{(0.508*s+1)(25504s^2-38.96s+1)}$	$-9.73 \cdot 10^{-10}\frac{(0.699s+1)(354.35s+1)(2282s+1)}{(0.508s+1)(25504s^2-38.96s+1)}$
α_{LM}	$0.0045\frac{(186.1s-1)(195.5s+1)}{(0.508*s+1)(25504s^2-38.96s+1)}$	$5.22 \cdot 10^{-13}\frac{(273.3s-1)(3.55\cdot 10^{7}s+1)}{(0.508*s+1)(25504s^2-38.96s+1)}$
α_{LT}	$0.026\frac{(184.48s+1)(185.78s-1)}{(0.508*s+1)(25504s^2-38.96s+1)}$	$4.047 \cdot 10^{-8}\frac{(255.17s-1)(2707s+1)}{(0.508*s+1)(25504s^2-38.96s+1)}$

Table B.4: Linearized around a choke-valve of 17.5 %

References

[1] J.G. Balchen, T. Andresen, and B.A. Foss. *Reguleringsteknikk*. Tapir trykk, 2004.

[2] K. Havre, K.O Stornes, and H. Stray. Taming slug flow in pipelines. *ABB Review*.

[3] H. Olsen. Anti-slug control and topside measurements for pipeline-riser system. Master's thesis, Norwegian University of Science and Technology, 2006.

[4] S. Skogestad and I. Postlethwaite. *Multivariable Feedback Control*. John Wiley & Sons, Ltd, 2005.

[5] E. Storkaas. *Stabilizing Control and Controllability: Control Solutions to avoid Slug Flow in Pipeline-Riser Systems*. PhD thesis, Norwegian University of Science and Technology, 2005.

[6] B. Venås. Sluggregulering i flerfase rør med riser ved hjelp av topp-side målinger. Master's thesis, Norwegian University of Science and Technology, 2006.